Multi-reflection process of extraordinary optical transmission in a single subwavelength metal slit

YUN-SONG ZHOU[1(a)], BEN-YUAN GU[2(b)], HUAI-YU WANG[3] and SHENG LAN[4]

[1] *Department of Physics, Capital Normal University - Beijing 100048, China*
[2] *Institute of Physics, Chinese Academy of Sciences - P.O. Box 603, Beijing 100080, China*
[3] *Department of Physics, Tsinghua University - Beijing 100084, China*
[4] *Laboratory of Photonic Information Technology School for Information and Optoelectronic Science and Engineering - Guangzhou, Guangdong 510006, China*

Abstract – The process of the light passing through a single subwavelength metal slit is analyzed by the finite-difference time-domain method. The simulation results show that the slit can be considered as an effective dielectric region sandwiched by two scattering regions at the two slit ends. Thus, the slit is analogous to a Fabry-Perot (FP) etalon consisting of a dielectric slab with high-reflection coatings on its two surfaces. A formula is presented to evaluate the phase shift caused by the amplitude transmissivity of the coatings.

The extraordinary optical transmission (EOT) [1] in metallic gratings or Young's double-slits structures [2–16] is governed by the cooperation of two basic effects: one is the single-slit effect and the other is the inter-slit effect [17]. The single-slit effect means that an isolated slit may enhance or suppress the transmission of the light passing through the slit [5,11]. The inter-slit effect enhances or suppresses EOT owing to the interference between two waves: one is the light that passes through the slit directly, and the other is the surface wave (or SPP wave) that is excited at the adjacent slit and transmitted along the metal surface [6,7,18]. As the SPP generation depends on the intensity of light in the slit, the properties of the light passing through a single slit should be more essential. Thus the key is to understand clearly the EOT mechanism in a single slit. In general, the single slit is treated theoretically as a Fabry-Perot (FP) cavity with two open ends [4,11,16]. However, it is believed that the single-slit effect is not comprehended very well so far [16,19]. The reason of the theoretical failures is that the physical process of EOT in a slit is not perfectly described.

In order to explore the transmission process accurately, in this letter, we employ the finite-difference time-domain (FDTD) method to simulate the light transmission through a subwavelength slit cut into the metal film in detail. The multi-reflection processes are clearly revealed. The multi-reflection effect can be described by a phenomenal model which is a FP cavity composed of a plated dielectric slab instead of the simple FP cavity usually considered.

We consider a slit drilled in a silver film as sketched in fig. 1(a). A TM-polarized light wave (with the magnetic field parallel to the slit) with the wavelength of $\lambda_0 = 0.8\,\mu$m illuminates the slit structure from below. The slit exit is covered by an ideal monitor which detects the light field but does not disturb it. All of the obtained results are picked up from the corresponding monitor placed at different positions. Here we only draw one monitor in fig. 1(a) as a demonstration. A Cartesian coordinate system is set as in fig. 1(a). The slit width and the film thickness, *i.e.*, the slit depth, are denoted as w and h, respectively. The transmission processes through the slit are simulated by FDTD method [20]. The simulation domain is encircled by perfectly matched layer condition. The refractive index of silver, $n_{Ag} = 0.036 + i5.586$ at $\lambda_0 = 0.8\,\mu$m, is obtained by fitting of the experimental data [21].

First, we simulate the electromagnetic wave transmission through a sample with $h = 2.0\,\mu$m and $w = 0.1\,\mu$m. The intensity distribution of the y-component of the

_____
[(a)]E-mail: `263zys@263.net`
[(b)]E-mail: `guby@aphy.iphy.ac.cn`
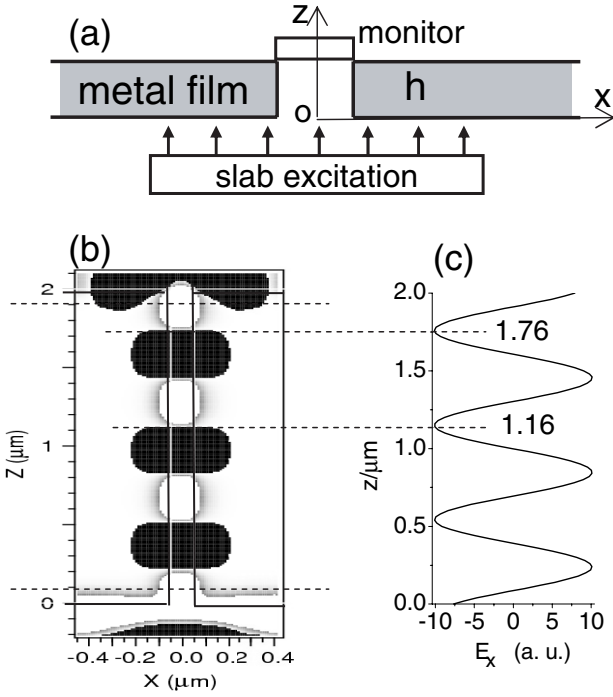
Fig. 1: (a) Sketch of the subwavelength metal slit illuminated by light wave from below. An ideal monitor is set on the slit exit. (b) The pattern of the magnetic field around the slit obtained by FDTD simulation. (c) The x-component of the electric-field distribution in the slit.

magnetic field around the slit is displayed in fig. 1(b), and the x-component of the corresponding electric field E_x, detected at the median plane ($x = 0$) of the slit is depicted in fig. 1(c). The two figures clearly show that the SPP wavelength in the slit is $\lambda_{SPP}^{slit} = 1.76 - 1.16 = 0.60\,\mu m$, which varies with w but is independent of h. As well known, the SPP wavelength at the $air(\epsilon_0)$/$metal(\epsilon_m)$ flat interface is given by $\lambda_{SPP} = \lambda_0\sqrt{(\epsilon_0 + \epsilon_m)/\epsilon_0\epsilon_m}$ [22]. Thus, in present case, we should have $\lambda_{SPP} = 0.787\,\mu m$, which is rather different from $\lambda_{SPP}^{slit} = 0.60\,\mu m$. This result prompts us to define an effective refractive index $n_{eff} = \lambda_0/\lambda_{SPP}^{slit} = 0.8/0.6 = 4/3$ for the slit of $w = 0.1\,\mu m$. It is worth noticing from fig. 1(b) that the magnetic field penetrates into the silver film from the two surfaces with the penetration depth about $\Delta h = 0.1\,\mu m$, as labeled by the dashed lines at the positions $z = 0.1$ and $1.9\,\mu m$, respectively. Therefore, there are two regions near the open ends of the slit with the same thickness Δh, in which the light will exhibit complicated behavior. Hereafter we refer the region near the entrance (exit) with thickness Δh to the first (second) scattering region. Consequently, the region sandwiched between the two dashed lines ($z = 0.1$ and $1.9\,\mu m$) in fig. 1(b) is referred to the effective dielectric region with a thickness h_{eff}, within which the effective refractive index is just n_{eff}. So the slit depth can be written as $h = h_{eff} + 2\Delta h$. In fig. 1(b), the effective dielectric region is between the dashed lines at $z = 0.1$ to $1.9\,\mu m$, so
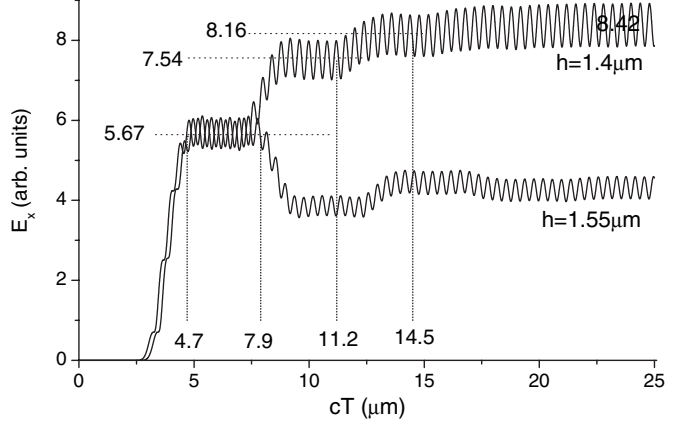
Fig. 2: Amplitude of the electric field varying with the sampling time. The curves labeled by $h = 1.4\,\mu m$ and $h = 1.55\,\mu m$ correspond to the sample with the corresponding slit depth.

that $h_{eff} \approx 1.8\,\mu m$. Our calculation results show that the value of Δh remains unchanged when the slit depth h is varied.

Hereafter the slit width is fixed at $w = 0.1\,\mu m$ for all calculations. The transmission processes of light through the slit are simulated. The curves shown in fig. 2 are the amplitudes of the x-component of electric fields detected by the monitor covered at the slit exit. The metal film thicknesses in this plot correspond to $h = 1.4\,\mu m$ and $1.55\,\mu m$, respectively. The abscissa is cT, where c is the velocity of light in vacuum and T the sampling time. It is assumed that the initial time of the radiation from the excited slab is set as $T = 0$. The curve of $h = 1.4\,\mu m$ exhibits a series of plateaus with an identical width of $c\Delta T = (14.5 - 4.7)/3 \approx 3.27$. In this time interval, the light in the slit should travel a distance of $\Delta d = c\Delta T/n_{eff} = 2.45\,\mu m$. Considering $h_{eff} = h - 2\Delta h \approx 1.4 - 0.2 = 1.2\,\mu m$, we have $2h_{eff} \approx \Delta d$. Therefore, in this time interval, the light travels a round-trip within the effective dielectric region. Thus, it may be conjectured that the actual physical process is as follow: when the TM-polarized light with the amplitude E_0 arrives at the slit entrance, it is scattered in the first scattering region and separated into two parts: one goes straightly into the dielectric region with the amplitude of E_0t and the other is reflected back with the amplitude of E_0r, where t (r) is the amplitude transmissivity (reflectivity) of the scattering regions defined as the ratio of the transmission (reflection) electric field to the incident field, both being the sum of all modes if there are more than one mode. The E_0t wave keeps on going forward and arrives at the second scattering region, and then scattered by the second scattering region. Therefore, the amplitude of the wave going out of the slit becomes E_0tt', where t' is the transmissivity when light goes out of the slit. The value of E_0tt' is just the altitude of the first plateau, 5.67, in fig. 2. Consequently, it is easily recognized that the second plateau of the curve of $h = 1.4\,\mu m$ in fig. 2 is determined by $E_0tt' + E_0tt'r^2$

(in phase). By analogy, the third plateau corresponds to $E_0 tt' + E_0 tt' r^2 + E_0 tt' r^4$, etc. This optical multi-reflection process resembles essentially to the case when the light perpendicularly transmits through a dielectric slab with the thickness h_{eff} and the refractive index n_{eff}.

In the same manner, the curve of $h = 1.55\,\mu m$ in fig. 2 is easily analyzed. Because in this case we have $2h_{eff} = 2 \times (1.55 - 0.2) = (4 + 1/2)\lambda_{SPP}^{slit}$, the out-phase interference occurs between the contiguously arriving transmission waves. This destructive interference results in the decline of the second plateau.

Our simulations show that the series of plateaus trend rapidly to a stable value as the sampling time is increased. It suffices to demonstrate that the difference of the altitudes between the fourth and the stable plateau (8.42 for $h = 1.4\,\mu m$) is negligible. The total transmission electric field can be expressed as

$$E_x^T = \mathrm{Re}\left[E_0 tt' \sum_{m=0}^{\infty} r^{2m} \exp(i2\pi 2mh_{eff}n_{eff}/\lambda_0) \right]. \quad (1)$$

According to the classical electrodynamics, the reflectivity of a dielectric slab is evaluated by $r = (n_{eff} - 1)/(n_{eff} + 1) \approx 0.142$. Unfortunately, when using this value in eq. (1), we obtain a result that deviates considerably from our simulation results. The reason is that a pure dielectric slab model is too simple to describe the behavior of the light in a metal slit, as it does not consider the effect of the scattering regions. We now employ a fitting method to get the amplitude reflectivity r. When $h_{eff} = 1.2\,\mu m$, $n_{eff} = 4/3$, and $\lambda_0 = 0.8\,\mu m$ are taken, eq. (1) becomes $E_x^T = E_0 tt' + E_0 tt' r^2 + E_0 tt' r^4 + \cdots$. From fig. 2 we have $E_0 tt' = 5.67$, $E_0 tt' + E_0 tt' r^2 = 7.45$, and $E_0 tt' + E_0 tt' r^2 + E_0 tt' r^4 = 8.16$. Thus the reflectivity is estimated by

$$r = \sqrt{[(E_0 tt' + E_0 tt' r^2) - E_0 tt']/E_0 tt'} \approx 0.574,$$

or

$$r = \sqrt[4]{[(E_0 tt' + E_0 tt' r^2 + E_0 tt' r^4) - (E_0 tt' + E_0 tt' r^2)]/E_0 tt'} \approx 0.575.$$

Thus, the average value is about $r = 0.575$. With the same method, the reflectivity of the slit with $h = 1.55\,\mu m$ is also calculated and the result is $r = 0.575$ too. This r value is greatly larger than that estimated from $r = (n_{eff} - 1)/(n_{eff} + 1) \approx 0.142$, which implies that the scattering regions possess much higher reflectivity. We thus can imagine that the slit is equivalent to a dielectric slab plated with thin high-reflectivity layers on its two surfaces, called as a plated dielectric slab (PDS).

When $r = 0.575$ is used, the total electric field E_x^T as a function of h is calculated by eq. (1) and plotted by the solid curve in fig. 3(a). On the other hand, the FDTD results are depicted by the open circles. The solid curve fits the open circles satisfactorily. Figure 3(b) manifests that the PDS is a suitable model to describe the behavior of light in metal slit.
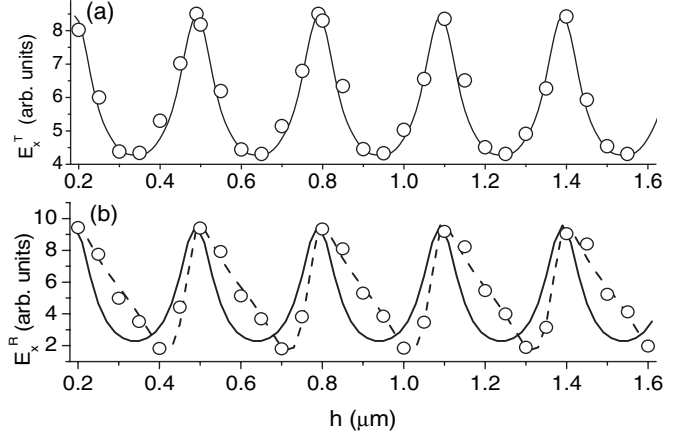
Fig. 3: Dependence of the total electric fields on the film thickness, (a) for transmission light field and (b) for light field just before the illuminated surface. The open circles represent the FDTD simulation results and the solid curve is calculated according to the multi-reflection theory in the PDS model. The dashed line is the corrected calculation result by introducing a phase shift.

To test the PDS model further, we now calculate the total field E_x^R just before the slit entrance, which includes the incident and reflection fields and is estimated by

$$\begin{aligned} E_x^R = {} & E_0(1 - r) \\ & + \mathrm{Re}\left[E_0 tt' \sum_{m=1}^{\infty} r^{(2m-1)} \exp(i2\pi 2mh_{eff}n_{eff}/\lambda_0) \right]. \quad (2) \end{aligned}$$

The minus sign before r in the first term comes from the π phase shift. The total field E_x^R calculated with eq. (2) is displayed by the solid curve in fig. 3(b). Our simulation results of E_x^R read from the monitor put on the slit entrance are represented by the open circles. All the parameters are the same as used in fig. 3(a). Both the solid curve and open circles display a perfect period of $\lambda_{SPP}^{slit}/2 = 0.3\,\mu m$, which provides a strong evidence of the multi-reflection process in the structure again. However, the solid curve does not exactly fit to the open circles. The lower circles shift rightward more. This reflects the fact that some physical processes may have been missed in eq. (2).

In order to find out the missed physical processes, let us explore the phase distribution of the light detected by a vertical monitor set in the slit at the position $x = 0.049$ that is very close to the slit wall and there exist the stronger electromagnetic field. The solid curve in fig. 4 demonstrates the phase distribution for the sample of $h = 1.4\,\mu m$ at the sampling time of $cT = 25\,\mu m$. The boundaries between the effective dielectric and the scattering regions are marked by the vertically dashed lines at $z = 0.1\,\mu m$ and $1.3\,\mu m$, respectively. In the dielectric region, the phase curve has two zero points located at $z = 0.7\,\mu m$ and $1.3\,\mu m$, respectively, from which we obtain the expected wave length $\lambda_{SPP}^{slit} = 0.6\,\mu m$. In the
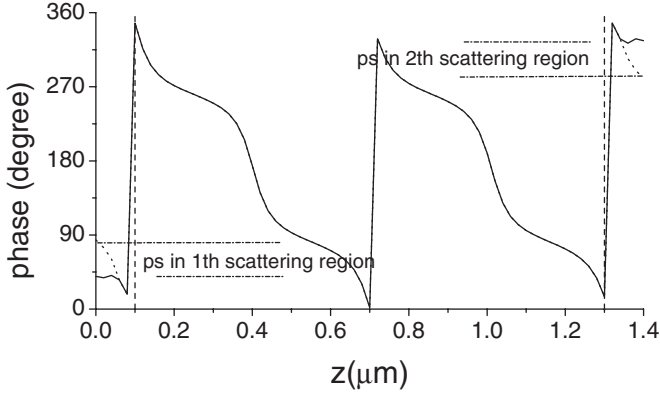
Fig. 4: Simulated phase distributions in the slit of $h = 1.4\,\mu m$.

Fig. 5: Sampling time dependence of the electric fields.

scattering regions, the curve exhibits an unusual behavior, which represents the transmission with phase shift (ps). The dotted curves in the two scattering regions are expected without the phase shift, which are drawn by shifting the corresponding sections of the solid curve around $z = 0.7$, for instance, the dotted curve in the second scattering region is shifted from the section of the solid curve located in the range from $z = 0.72$ to 0.8. Figure 4 shows that the phase shifts in the two scattering regions are equal. So the amplitude transmissivity of the scattering regions should yield a phase shift. Thus,

$$t = t_0 \exp(-i\theta_{ps}),$$
$$t' = t'_0 \exp(-i\theta_{ps}), \tag{3}$$

where t_0 and t'_0 are real numbers, and θ_{ps} is the phase shift in the unit of radian.

Now we investigate the phase shift in detail. Figure 5 displays the FDTD results detected by the monitor put on the slit entrance for the samples of $h = 1.4$ and 1.55, respectively. The curve of $h = 1.4$ should accord with the result calculated by eq. (2) when $h = 1.4$, *i.e.*, $E_x^R = E_0(1-r) + E_0 t t'(r + r^3 + r^5 + \cdots)$, so the first and second plateaus of the curve $h = 1.4$ correspond to the first and second terms of eq. (2), respectively. They are $\mathrm{Re}[E_0(1-r)] = 4.73$, and $\mathrm{Re}[E_0(1-r) + E_0 t t' r] = 7.43$. From the two equations and using $r = 0.575$ we obtain $\mathrm{Re}(E_0 t t') = \mathrm{Re}[E_0 t_0 t'_0 \times \exp(-i2\theta_{pl})] = (7.43 - 4.73)/0.575 \approx 4.69$. It is evident from eq. (1) that the phase shift cannot influence the interferences between the transmission waves. Consequently, $E_0 t t' = 5.67$ obtained from fig. 2 should be rewritten as $E_0 t_0 t'_0 = 5.67$. Combination of $\mathrm{Re}[E_0 t t' \exp(-i2\theta_{ps})] \approx 4.69$ and $E_0 t_0 t'_0 = 5.67$ leads to $\theta_{ps}^{in} \approx 17\pi/180$, where the superscript "in" means that the value corresponds to the in-phase interference. In the same way we acquire $\theta_{ps}^{out} \approx 40\pi/180$, which corresponds to the out-phase interference from the curve associated with the sample of $h = 1.55\,\mu m$ in fig. 5. The difference between θ_{ps}^{in} and θ_{ps}^{out} indicates that the phase shift is related to the FP resonant cavity, which depends on the
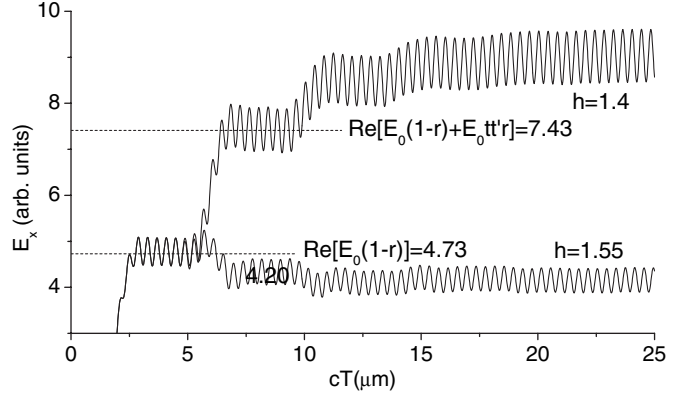
film thickness. This fact implies that the SPP generations at the entrance and exit are influenced each other. In other words, the phase shift reflects the coupling effect between the SPP generations in two scattering regions.

Based on the analysis above, we propose a formula to calculate the phase shift,

$$\theta_{ps} = \theta_{ps}^{in} + (\theta_{ps}^{out} - \theta_{ps}^{in})|\sin(2\pi h_{eff} n_{eff}/\lambda_0)|. \tag{4}$$

The calculated total field before entrance when the phase shift is considered by eq. (4) is plotted by the dashed curve in fig. 3(b), which coincides with the FDTD results very well.

Lastly, we compare more explicitly the PDS model with a simple FP cavity and the corresponding theory. As the FP resonant condition is given by the equation $n\lambda_{FP} = 2h$, where n is an integer. It is seen from fig. 3 that the thickness $h = 1.4\,\mu m$ just corresponds to a FP resonant peak if the metal slit is thought as a simple FP cavity. Since $\lambda_{FP} = 0.8\,\mu m$, we get $n = 3.5$, which is not an integer. The failure indicates that a FP cavity is too simple to describe the light behavior in a metal slit. Takakura [16] has noticed the difference between a FP cavity and a narrow metal slit structure and introduced a shift of a resonant wavelength λ_{shift} to try to meet the resonant condition. We get $\lambda_{shift} = 0.083\,\mu m$ by the formula in ref. [16] with $h = 1.4\,\mu m$, and $w = 0.1\,\mu m$. This value, combined with the resonant condition $n\lambda_{FP} = 2h$, yields $n = 2.72$, which is not an integer once more. Another contradiction appeared is that the modified resonant wave length $\lambda_{modified} = \lambda_{FP} + \lambda_{shift} = 0.883\,\mu m$ is even larger than λ_{FP}, while the real resonant wave length should be $\lambda_{SPP}^{slit} = 0.6\,\mu m$. Thus we believe that a simple FP cavity, even a modified one, cannot describe the real EOT processes accurately.

In summary, in terms of the FDTD simulations we find that a single metal slit can be modeled by an effective dielectric slab coated by high-reflective coatings on its two surfaces (PDS model). The multi-reflection occurs in the effective dielectric region. The transmissivity of the coating not only weakens the amplitude of the transmission field, but also causes the phase shift.

A formula to evaluate the phase shift is presented, and the results calculated by the formula reach a satisfactory agreement with the FDTD simulations. It is believed that our model may provide a useful avenue to investigate the EOT effect in an intuitionistic physical picture.

* * *

REFERENCES

[1] Ebbesen T. W., Lezec H. J., Ghaemi H. F., Thio T. and Wolff P. A., *Nature (London)*, **391** (1998) 667.

[2] Ghaemi H. F., Thio T., Grupp D. E., Ebbesen T. W. and Lezec H. J., *Phys. Rev. B*, **58** (1998) 6779.

[3] Schröter U. and Heitmann D., *Phys. Rev. B*, **58** (1998) 15419.

[4] Porto J. A., Garcia-Vidal F. J. and Pendry J. B., *Phys. Rev. Lett.*, **83** (1999) 2845.

[5] Lalanne P., Hugonin J. P. and Rodier J. C., *J. Opt. Soc. Am. A*, **23** (2006) 1608.

[6] Schouten H. F., Kuzmin N., Dubois G., Visser T. D., Gbur G., Alkemade P. F. A., Blok H., 't Hooft G. W., Lenstra D. and Eliel E. R., *Phys. Rev. Lett.*, **94** (2005) 053901.

[7] Lalanne P., Hugonin J. P. and Rodier J. C., *Phys. Rev. Lett.*, **95** (2005) 263902.

[8] Nikitin A. Yu., Lopez-Tejeira F. and Martin-Moreno L., *Phys. Rev. B*, **75** (2007) 035129.

[9] Treacy M. M. J., *Appl. Phys. Lett.*, **75** (1999) 606.

[10] Treacy M. M. J., *Phys. Rev. B*, **66** (2002) 195105.

[11] Cao Q. and Lalanne P., *Phys. Rev. Lett.*, **88** (2002) 057403.

[12] Barbara A., Que'merais P., Bustarret E., Lo'pez-Rios T. and Fournier T., *Eur. Phys. J. D*, **23** (2003) 143.

[13] Hibbins A. P., Lockyear M. J. and Sambles J. R., *J. Appl. Phys.*, **99** (2006) 124903.

[14] Visser T. D., *Nat. Phys.*, **2** (2005) 509.

[15] Aigouy L., Lalanne P., Hugonin J. P., Julie G., Mathet V. and Mortier M., *Phys. Rev. Lett.*, **98** (2007) 153902.

[16] Takakura Y., *Phys. Rev. Lett.*, **86** (2001) 5601.

[17] Zhou Y. S., Gu B. Y., Lan S. and Zhao L. M., *Phys. Rev. B*, **78** (2008) 081404(R).

[18] Liu H. and Lalanne P., *Nature*, **452** (2008) 728.

[19] Suckling J. R., Hibbins A. P., Lockyear M. J., Preist T. W., Sambles J. R. and Lawrence C. R., *Phys. Rev. Lett.*, **92** (2004) 147401.

[20] Yee K. S., *IEEE Trans. Antennas Propag.*, **14** (1966) 302; in this letter, a commercially available software developed by Rsoft Design Group (`http://www.rsoftdesign.com`) is used for the numerical simulations.

[21] Johnson P. B. and Christy R. W., *Phys. Rev. B*, **6** (1972) 4370.

[22] Raether H., *Surface Plasmons on Smooth and Rough Surfaces and on Gratings* (Springer-Verlag, Berlin) 1988.